ACTIVATION AND DECAY CHARACTERISTICS OF RADIATION SHIELDING HEAVY CONCRETES

By

É. M. ZSOLNAY, GY. CSOM and E. J. SZONDI

Nuclear Training Reactor of the Technical University, Budapest

1. Introduction

The most important radiation shielding units of a nuclear power plant are the ones surrounding the reactor vessel. These structures are produced of special concretes and become radioactive due to neutron irradiation during the operating life of the reactor. The radionuclides produced are in most cases γ-radiation emitters, consequently they will give a contribution to the dose rate developing on the surface and inside of the shielding during and after the reactor operation. Nevertheless, the maintenance of the nuclear power plant requires that special parts of the reactor should be approachable in a short time after shutdown at the end of an operational period.

On the other hand, nuclear power reactors will eventually reach the end of their useful life, and it will be necessary to provide for the decomposition of these facilities. The decommissioning of retired nuclear power plants is a subject that is recently receiving international attention [1]. From the limited experiences and studies available in this field so far [1—4], it is clear that serious technical problems arise from the decomposition, removal, transportation, protective storage and entombment of radioactive wastes and structure materials of a nuclear facility, and the costs associated with decommissioning are also significant.

Table 1 shows the approximate weight of the construction materials for two different reactors [4]. From these data it is seen that the reactors are surrounded by more thousands of tons of shielding concretes. The quantities of activation products produced in the concrete structures adjacent to the reactor vessel are dependent on their composition. As this may vary from reactor to reactor it will be necessary to analyse the actual activated concrete for the reactor in question to obtain an accurate estimate of the activities present. Ideally, planning for maintenance and decommissioning should be considered at the design stage of the facility.

In Hungary, the first nuclear power plant has been under construction. The operation of the first reactor block will be started in 1982, and it will be

Table 1

Approximate weight of construction materials (tonnes) of two different reactors

Item	WAGR			
	Mild steal	Stainless steel	Graphite	Concrete
1. PV and internals	600	40	300	
2. Biological Shield	200			4000
3. Heat	150 each			
Exchangers	(4-off)			

Item	Commercial MAGNOX station			
	Mild steel	Stainless steel	Graphite	Concrete
1. PV and internals	2500	100	2500	
2. Biological Shield	800			16 000
3. Heat	345 each			
Exchangers	(4-off)			

followed by three additional blocks. The shielding problems of these blocks will have to be solved by sources and capacities available within the country. Therefore an extended program was financed by the Ministry of Building Affairs for development of special concretes to be used in the radiation shielding structures of the nuclear power plant. In frame of this work 4 kinds of shielding heavy concretes have been developed by the Institute for Building Science Budapest (ÉTI) and investigated by the Nuclear Training Reactor of the Technical University Budapest from the point of view of shielding and activation properties [5—11].

In this paper the studies relating to the activation properties and the results obtained will be presented.

2. Determination of the activation properties of shielding heavy concretes

The aim of the investigations was to study the activation and decay characteristics of some shielding heavy concretes having favourable neutron and gamma attenuation properties, and to find the optimal composition of aggregates from both shielding and activation points of view. For this purpose the following parameters related to the secondary γ-radiation of the irradiated concretes have been determined:

— The change of gamma dose rate on the surface of the shielding concretes during and after the operating life of the reactor,

— The specific activity — and its most important components — in the concrete after the final shutdown of the nuclear power plant.

These quantities will determine the conditions of accessibility of special places

within the shielding structure during the maintenance and after the final shutdown of the reactor and the criteria of decomposition of the shielding structures. From both points of view the presence of radioisotopes with short half life would be preferable.

The solution of the problem involved the following steps:

· 1) The chemical composition of the concretes was determined.

2. A special computer code CAP was developed for the calculation of the desired quantities [25].

3) The calculations were executed under different conditions.

4) The results obtained were analysed and requirements of producing radiation shielding concretes with optimal activation characteristics were summarized.

2.1 *Composition*

The investigated concretes were iron-aggregated heavy concretes, namely:

— iron-siderite,

— iron-hematite I,

— iron-hematite II, and

— iron-limonite

concretes. The mix composition of the concretes is given in Table 2 [12, 13, 24]. The iron aggregate was involved in the concretes in form of steel shot.

The concrete iron-hematite I contained unclassified hematite deriving from the mine of Krivoi Rog (S.U.) while in case of the concrete iron-hematite II a part of the Krivoi Rog hematite was substituted by a special Brazilian hematite classified by grain size having greater density than the Krivoi Rog one. The aim of using Brazilian hematite aggregate was to decrease the quantity of the expensive steel shot in the concrete in coincidence with keeping (or improving) the original shielding ability and improving the activation characteristics of the concrete in question. The effect of this modification will be discussed later-on.

The samples to be investigated were taken from the trial dies used in the radiation shielding experiments. As the ratio of the steel shot in the concrete was rather high in all cases, this aggregate was separated from the other concrete components and the samples obtained this way were analysed.

The chemical composition of the samples was determined using the multi-comparator method of the neutron activation analysis [14—16]. The results obtained are shown in Table 3. Only those concrete components are seen in the Table which could be detected by the method of the neutron activation analysis. The elements not detectable this way — just because they are not

Table 2

The mix composition of the investigated radiation shielding concretes

Concrete	Composition	Partial density [kg/m^3]	
Iron-siderite	Lábatlan cement	360	
	350 ppc. 10		
	Siderite	1676	
	Steel shot	1622	
	Water + plastificator	190	
	Total		3848
Iron-limonite	Tata cement	286	
	350-K ppc. 10		
	Limonite	1487	
	Steel shot	1626	
	Water + plastificator	167	
	Total		3986
Iron-hematite I.	Lábatlan cement	380	
	350 ppc. 10		
	Hematite (of Krivoi Rog)	1771	
	Steel shot	1626	
	Water + plastificator	209	
	Total		3986
Iron-hematite II.	Beremend cement	395	
	350 ppc. 10		
	Hematite (of Krivoi Rog)	930	
	Hematite (Brazilian)		
	6—24 mm	1400	
	Steel shot	995	
	Water	186	
	Plastificator	12	
	Total		3918

sensitive for this method — are not important (or much less important than the presented ones) from the point of view of activation.

The data in Table 3 show the elementary composition of the complete concretes in question, that is the components of the steel shot aggregate are also involved. Nevertheless, the elementary composition of this aggregate has also been analysed and the results obtained are presented in Table 4. The most frequent alloying elements — such as Cr, Ni and Co — the half life of the radioisotopes of which is rather long could not be detected. As a result, we may conclude the steel shot aggregate used in the investigated samples had been produced of unalloyed steel.

Table 3

Chemical elements in the concrete samples and their concentration (in weight per cent)

Element	Iron-siderite concrete [%]	Iron-hematite I. concrete [%]	Iron-limonite concrete [%]	Iron-hematite II. concrete [%]
Na	0.57	0.08	0.49	0.0431
Mg	2.70	2.2	2.2	—
Al	1.70	2.2	1.6	1.2173
Sc	0.0002	0.0003	0.0003	0.0002
V	0.002	0.003	0.0035	0.0043
Cr	0.26	0.026	0.028	0.0197
Mn	0.95	0.22	1.49	0.1975
Fe	55.80	70.80	72.30	57.72
Co	0.0005	0.0007	0.0004	0.0012
As	0.0011	0.0011	0.031	0.0047
Sb	0.004	0.0002	0.004	0.0002
Ba	10.30	0.035	1.00	—
La	0.0018	0.0014	0.0011	0.0008
Ce	0.0015	0.0028	0.0022	—
Eu	0.0001	0.0001	0.0001	0.0001
Hf	0.0018	0.0001	0.0001	—
Th	0.0003	0.0004	0.0002	—
Pa	—	—	—	0.0002

The uncertainty in the concentration values is less than 6% in every case

Table 4

Chemical elements in the steel shot aggregate and their concentration in the concrete (weight per cent)

Element	Concentration [%]
V	0.0020
Mn	0.1124
Cr	0.0105
Fe	23.3683
Na	0.0023
As	0.0044
Sb	0.0001
Co	0.0009

The uncertainty in the concentration values is less than 6% in every case

4*

Two of the shielding concretes (iron-siderite and iron-limonite) had been designed with a given barium content to increase their density and radiation shielding ability. Another important difference between the four kinds of heavy concretes from point of view of composition was found in their iron-content being also the result of preliminary design. Their influence on the activation characteristics will be discussed in Chapter 3.

2.2 *Calculations*

2.2.1. The computer program CAP

A computer code (CAP = Calculation of Activation Properties) has been developed to determine the activation properties of the shielding concretes [25]. The main characteristics of this program are as follows:

1) *The physical model of the activation-decay procedure*

— In case of qualifying the different concretes the complete operating life ($\sim 30-40$ years) of the reactor has to be considered. During such a long time the elementary composition of the shielding concrete will be changed by neutron induced nuclear transmutations. Taken into account the usual chemical elements in the concrete (see Table 3) and the neutron flux densities present in the shielding structures the activation-decay process presented by Fig. 1 has been studied. The reaction- and decay-products not indicated in this figure have been neglected.
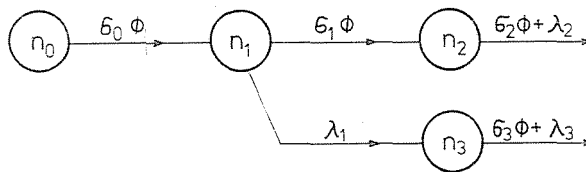
Fig. 1. Activation-decay processes studied in case of the investigated heavy concretes

— In the surroundings of nuclear reactors the neutron flux density is space- and time-dependent. This circumstance has been taken into account by the following simple assumptions:

a) the spatial distribution of the neutron flux density in the concrete can be given by series of exponential functions;

b) during the activation the neutron flux density at a given point of the concrete is constant in time.

2) *Mathematical model of the activation-decay procedure*
The reaction rate for the i-th target nuclide can be written as

$$R_i = \int_0^\infty \sigma_i(E)\Phi(E)\,\mathrm{d}E \tag{1}$$

where

$\sigma_i(E)$ is the energy dependent cross section for the reaction of interest

$\Phi(E)$ is the neutron flux density per unit energy interval. Approximating this integral equation by integration formula one obtains:

$$R_i = \sum_{j=1}^m \sigma_{ij}\Phi_j \tag{2}$$

where m is the number of energy groups in the cross section library.

Introducing a virtual decay constant the diminution by neutron capture and spontaneous decay of the i-th nuclide in the concrete can be given as

$$\Lambda_i = \sigma_i\Phi + \lambda_i \tag{3}$$

where

Λ_i is the virtual decay constant

λ_i is the decay constant

σ_i and Φ are the symbols of the corresponding cross sections and the neutron flux density, respectively.

Using the symbols of Eq. (3) and Fig. 1, the time-dependent change of the i-th concrete component and its daughter products can be written as

$$\frac{\mathrm{d}n_{0i}}{\mathrm{d}t} = -n_{0i}\Lambda_{0i}$$

$$\frac{\mathrm{d}n_{1i}}{\mathrm{d}t} = n_{0i}\sigma_{0i}\Phi - n_{1i}\Lambda_{1i}$$

$$\tag{4}$$

$$\frac{\mathrm{d}n_{2i}}{\mathrm{d}t} = n_{1i}\sigma_{1i}\Phi - n_{2i}\Lambda_{2i}$$

$$\frac{\mathrm{d}n_{3i}}{\mathrm{d}t} = n_{1i}\lambda_{1i} - n_{3i}\Lambda_{3i}$$

As $\lambda_{0i} = 0$, $\Lambda_{0i} = \sigma_{0i}\Phi$.

This differential equation system has to be solved by the following initial assumptions:

$$n_{0i}(0) = n_{00i}$$

$$n_{1i}(0) = n_{2i}(0) = n_{3i}(0) = 0$$

The solution gives the space-dependent concentration of the γ-radiation emitter radionuclides in the concrete, to be used as input data to the γ-dose rate calculations.

3) *Calculation of the γ-dose-rate*

a) The γ-dose-rate is calculated by the program for the surfaces of the shielding wall using point kernel method completed with buildup factors [26].

b) The γ-photons are divided by energy into 8 groups as given in Table 5.

Table 5

Grouping of γ-photons by energy

Group number	Energy limit [MeV]	
	Lower	Upper
j	E_{j-1}	E_j
1	0	0.5
2	0.5	1
3	1	2
4	2	3
5	3	4
6	4	5
7	5	7
8	7	9

4) *Geometry*

As the aim of the calculations was determining material characteristics — and not investigating actual geometrical structures — one dimensional model with infinite plate geometry was used.

2.2.2. Input data

1) The calculations were performed under the following conditions:

a) From among the nuclear reactions leading to radioactivity only the neutron induced reactions were considered due to the larger probability of their production.

b) Within the neutron induced nuclear reactions the activities deriving from the slow neutron capture reactions were determined as

— the cross section of these reactions is much larger for the elements present in the concrete than that one for other (e.g. fast neutron induced) reactions. An exception in this respect may be the inelastic scattering of the fast ·neutrons on certain nuclides (e.g. iron, etc.), but for these events see the next statement:

— the fast neutron flux density reaching the surface of the shielding concrete is less with orders of magnitude than the thermal or intermediate one in that point [17].

c) Due to the above mentioned reasons two neutron energy groups — thermal and intermediate — were considered with the following boundaries:

thermal region $E_n \leq 0.2$ eV

intermediate region 0.2 eV $< E_n \leq 500$ keV

where E_n denotes the actual neutron energy.

d) The neutron spectrum calculated for the outer surface of the reactor vessel of the Paks Nuclear Power Plant (PWR) was taken as input spectrum [17].

e) The elements in the concretes could not be detected by reactor neutron activation (e.g. H, O, etc.) were taken into account in accordance with the mix composition and literature data referring to the composition of the corresponding heavy iron concretes [18].

2) Nuclear data:

A special nuclear data library has been compiled for the calculations containing the corresponding data (such as isotope abundances, half lives, neutron activation cross sections, γ-yields, γ-attenuation coefficients, γ-flux to dose rate conversion factors, etc.) for 144 reactions of 128 isotope nuclides [19–23]. The neutron attenuation within the concrete was calculated using the experimentally determined relaxation lengths for the concrete in question [5–7].

2.2.3. Results

The parameters calculated for the different kinds of concretes are as follows:
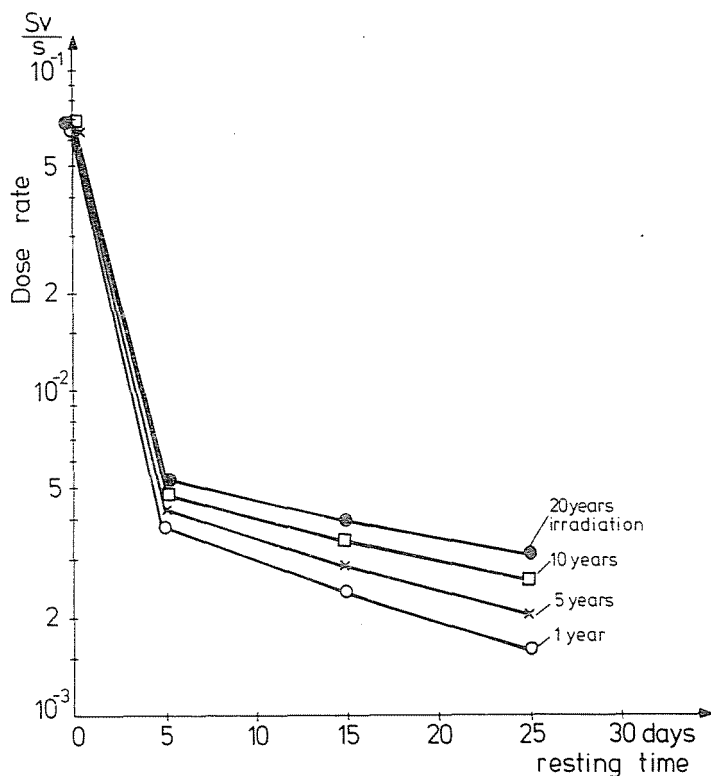
— dose rate on the neutron source side of the shielding concrete wall in function of the irradiation and resting time (in case of saturation wall thickness),
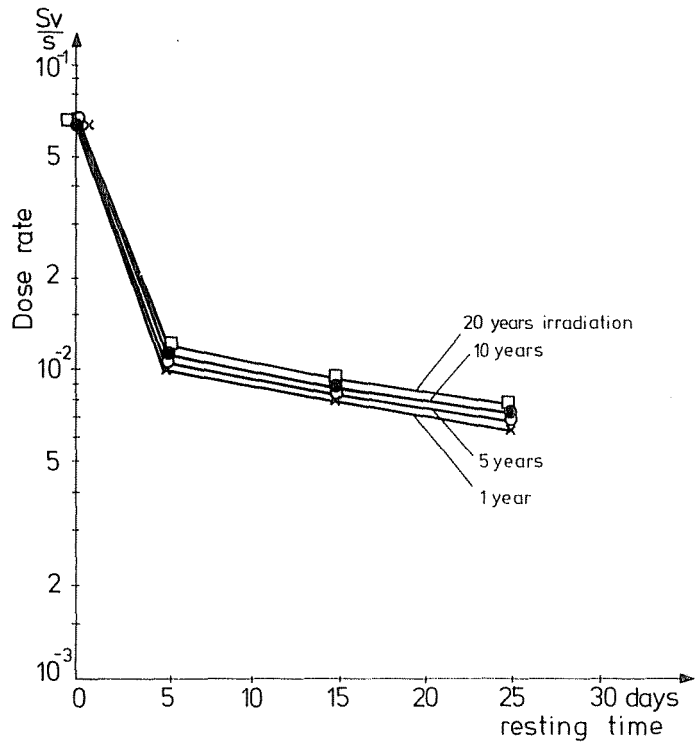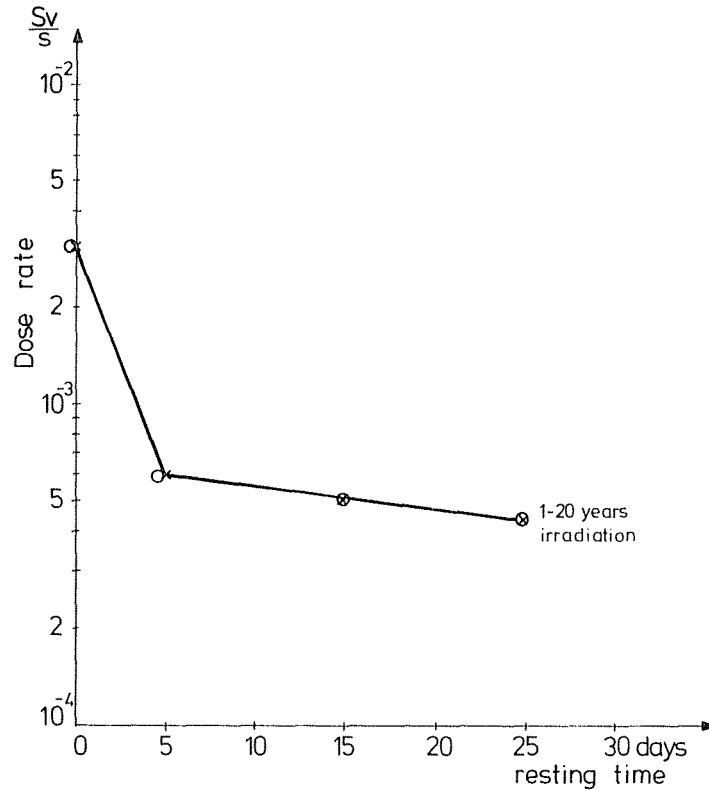
— specific activity — and its components — in the shielding concrete after 30 years operating life of the reactor as a function of the place within the concrete wall (resting time $= 0$),
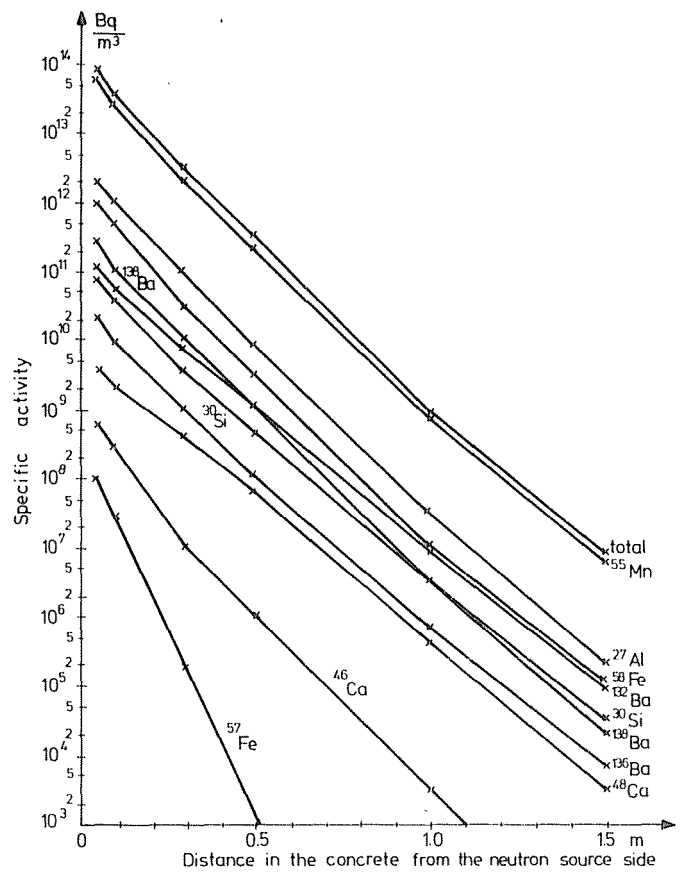
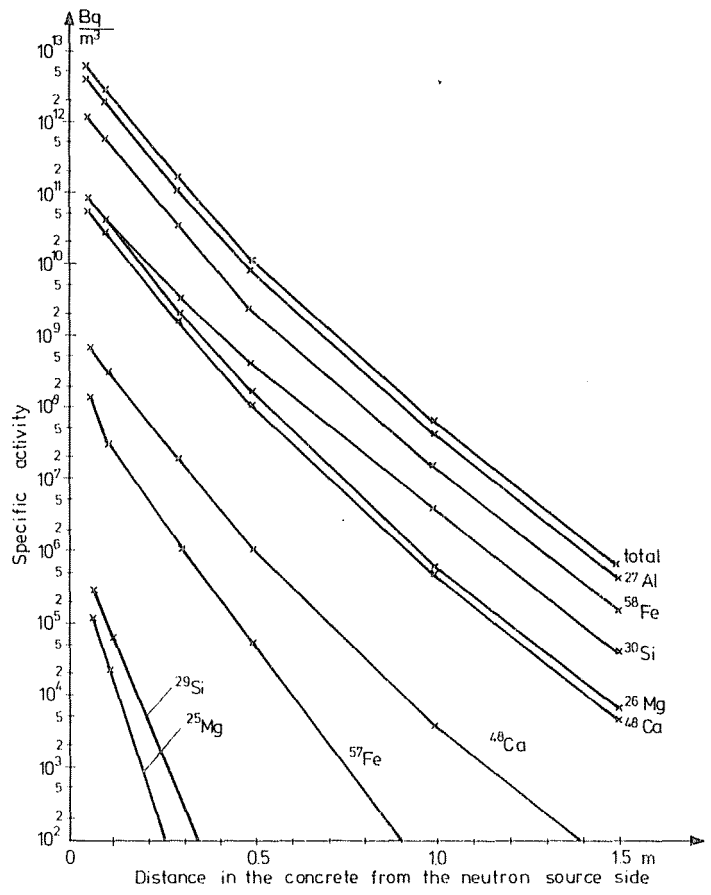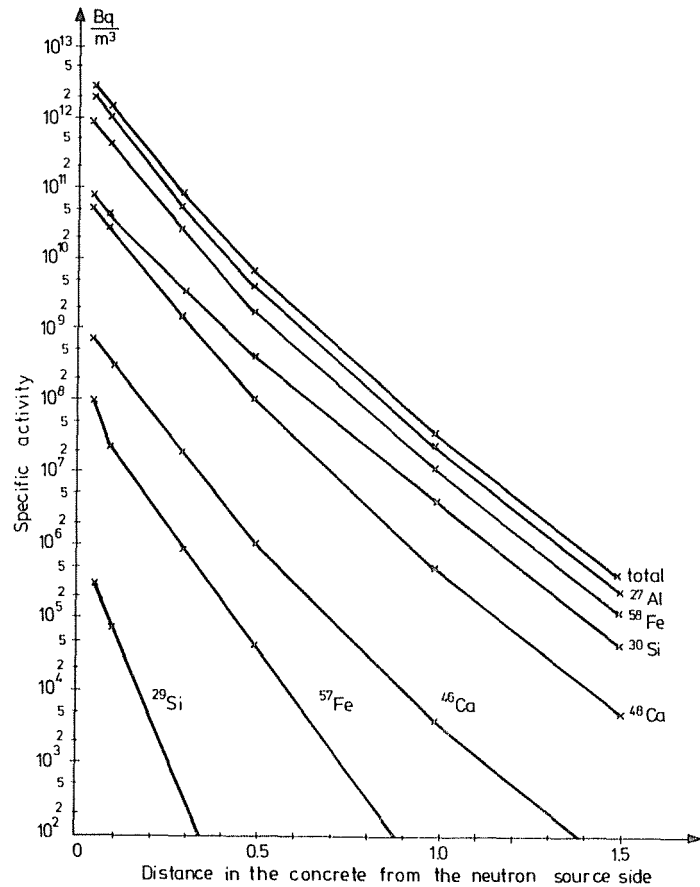— dose rate on the neutron source side of the shielding concrete wall after 30 years operating life of the reactor as a function of the shielding wall thickness and the resting time (resting time $= 0$, 1, 5 years),

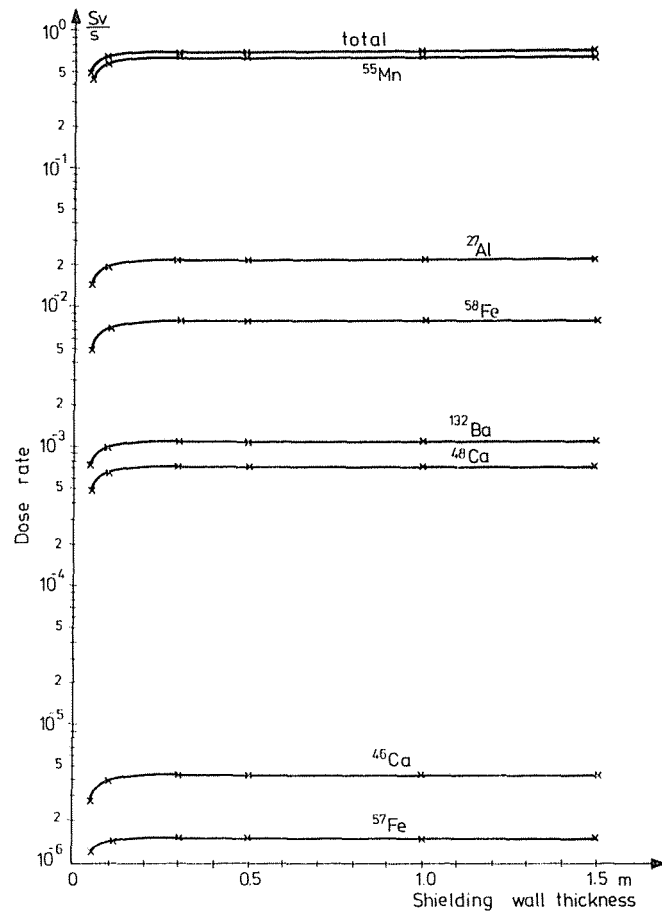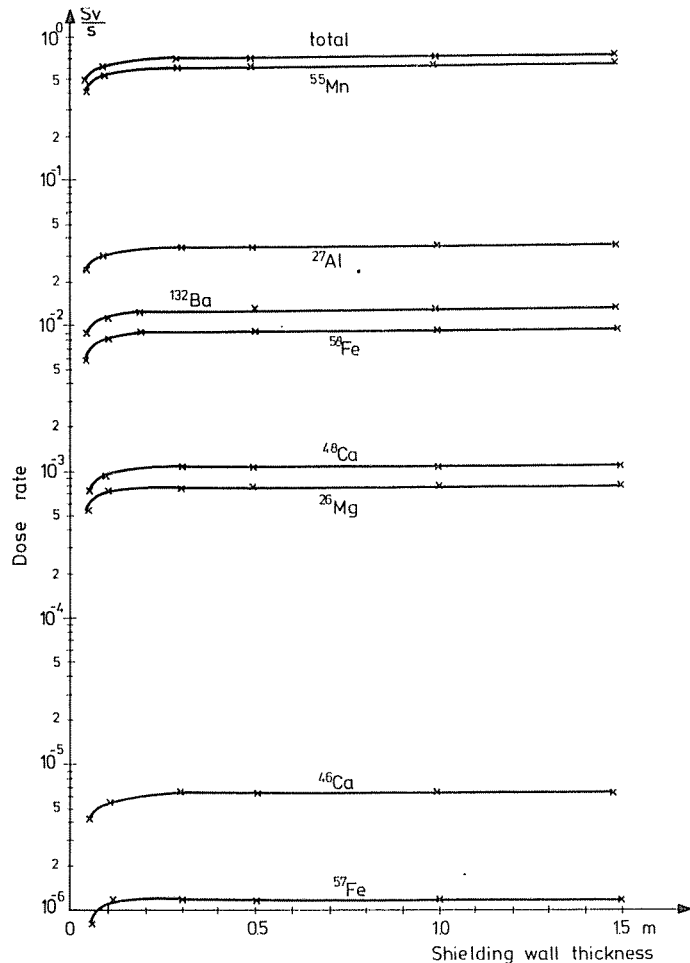— dose rate on the neutron source side of the shielding concrete wall after 30 years operating life of the reactor as a function of the resting time (in case of saturation wall thickness),

— dose rate on the shielded side of the concrete wall after 30 years operating life of the reactor as a function of the shielding wall thickness and the resting time.

The quantities listed above have been determined for both the concrete as a whole and its most important elementary components. The results obtained are shown in Figures 2–32. The contribution of the different elements in the concrete to the activity and dose rate is indicated by the inactive component of the corresponding activation-decay series.

Fig. 2. Dose rate on the neutron source side of the iron-siderite concrete wall as a function of the irradiation and resting time (in case of saturation wall thickness)

Fig. 3. Dose rate on the neutron source side of the iron-limonite concrete wall as a function of the irradiation and resting time (in case of saturation wall thickness)

Fig. 4. Dose rate on the neutron source side of the iron-hematite I concrete wall (after 1—20 years irradiation time) as a function of the resting time (saturation wall thickness)
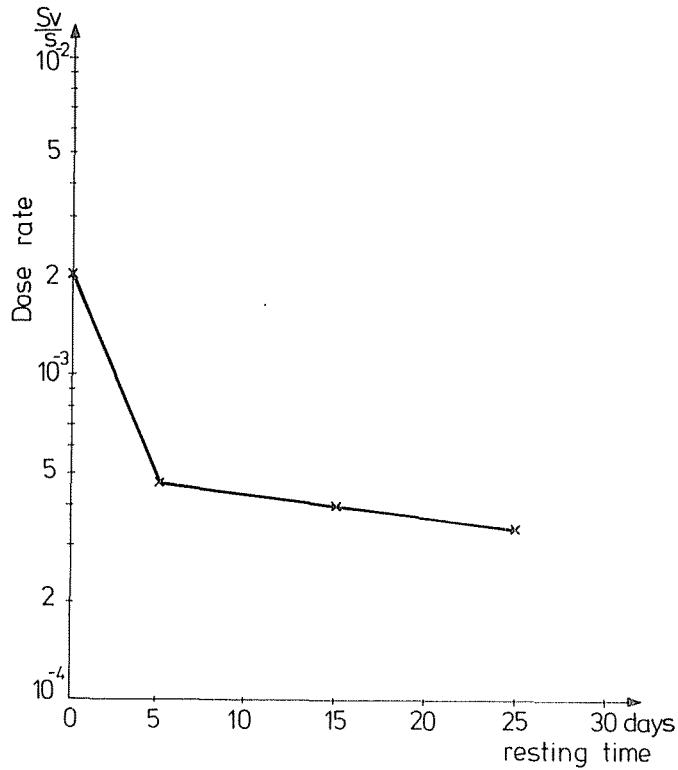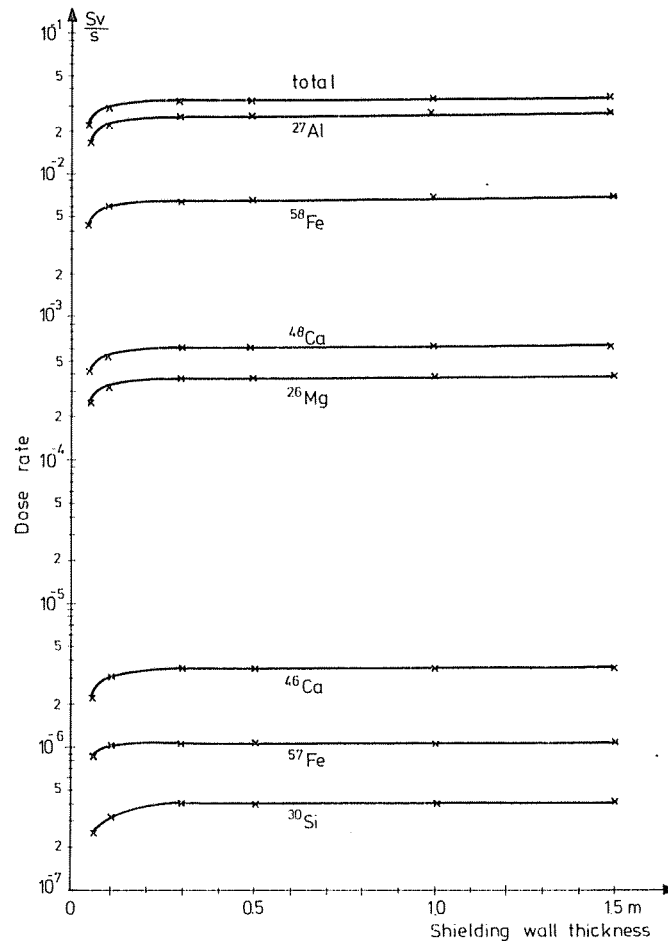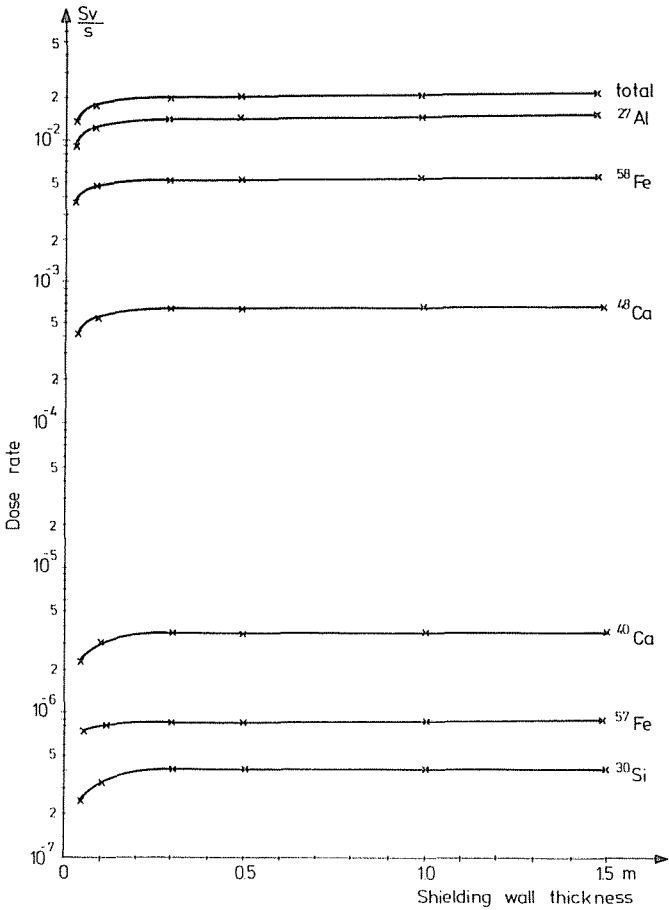
Fig. 5. Dose rate on the neutron source side of the iron-hematite II concrete wall (after 1—20 years irradiation time) as a function of the resting time (saturation wall thickness)
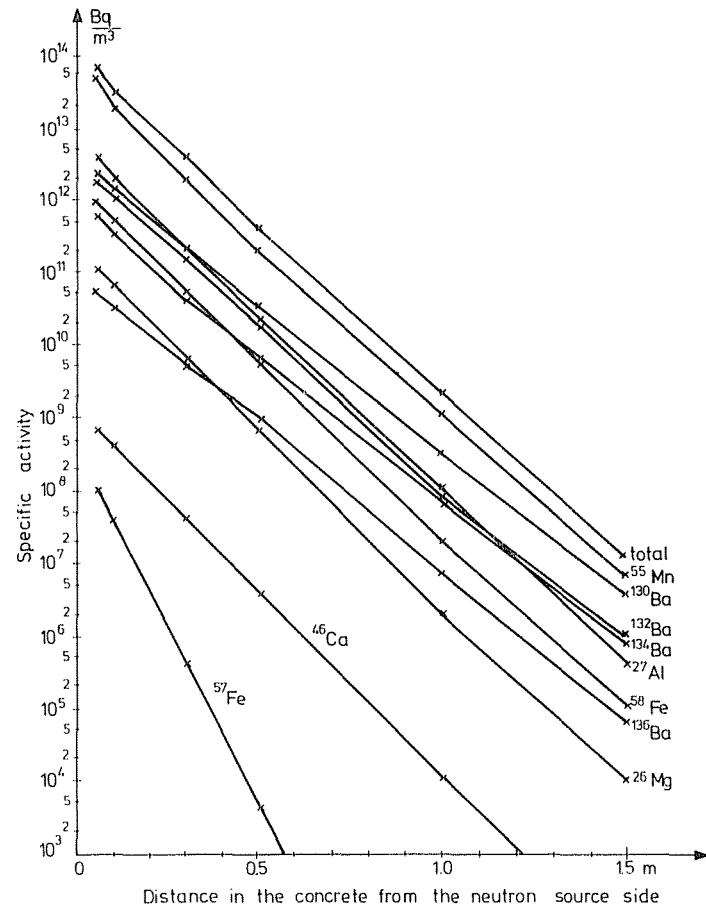
Fig. 6. Specific activity of the iron-siderite concrete after 30 years operating life of the reactor as a function of the place within the concrete wall (resting time = 0)

Fig. 7. Specific activity of the iron-limonite concrete after 30 years operating life of the reactor as a function of the place within the concrete wall (resting time = 0)

Fig. 8. Specific activity of the iron-hematite I concrete after 30 years operating life of the reactor as a function of the place within the concrete wall (resting time = 0)
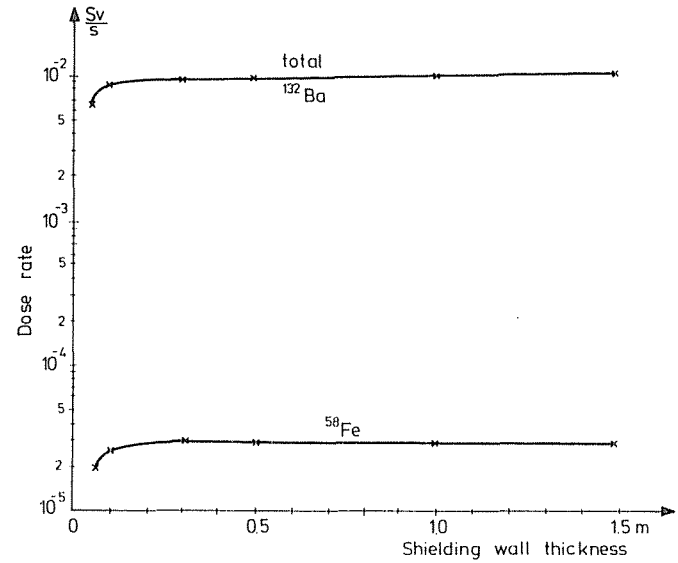
Fig. 9. Specific activity of the iron-hematite II concrete after 30 years operating life of the reactor as a function of the place within the concrete wall (resting time = 0)

Fig. 10. Dose rate on the neutron source side of the iron-siderite concrete wall after 30 years operating life of the reactor as a function of the shielding wall thickness (resting time = 0)
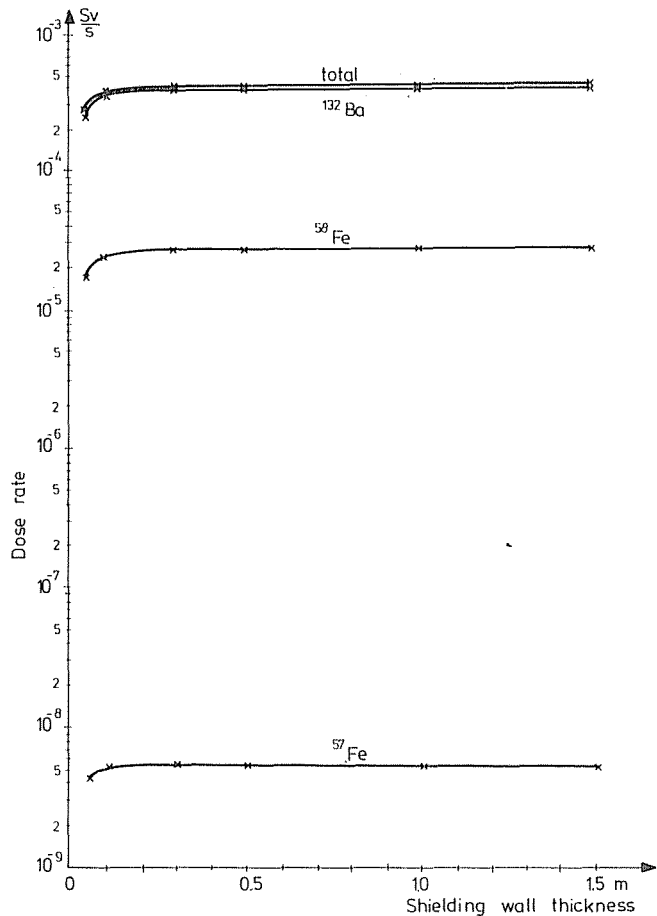
Fig. 11. Dose rate on the neutron source side of the iron-limonite concrete wall after 30 years operating life of the reactor as a function of the shielding wall thickness (resting time = 0)
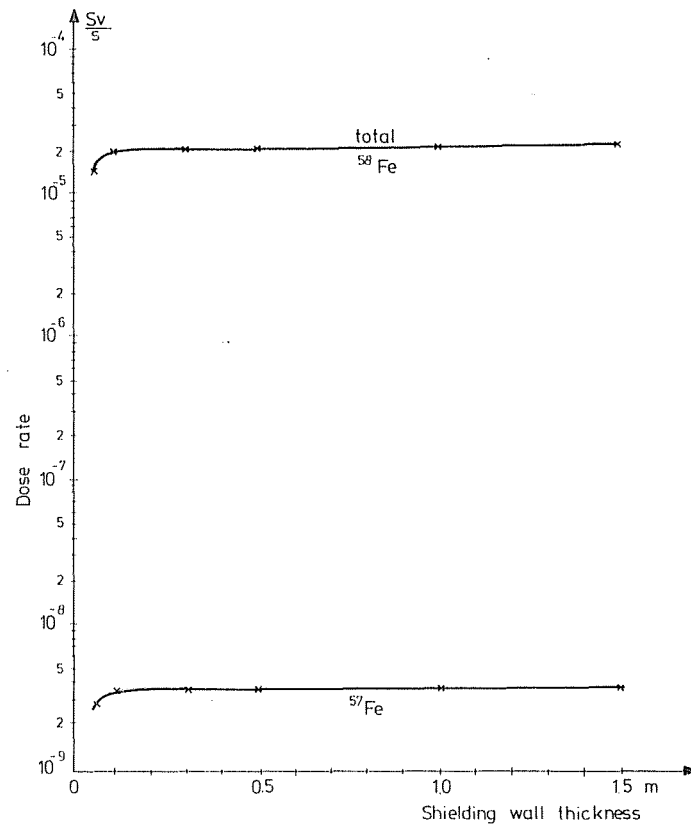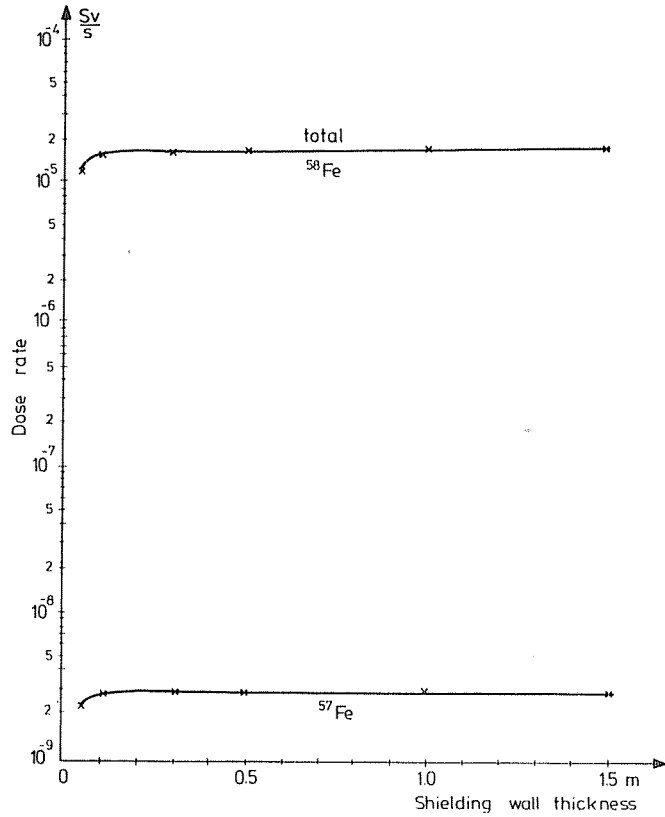
Fig. 12. Dose rate on the neutron source side of the iron-hematite I concrete wall after 30 years operating life of the reactor as a function of the shielding wall thickness (resting time = 0)

Fig. 13. Dose rate on the neutron source side of the iron-hematite II concrete wall after 30 years operating life of the reactor as a function of the shielding wall thickness (resting time = 0)
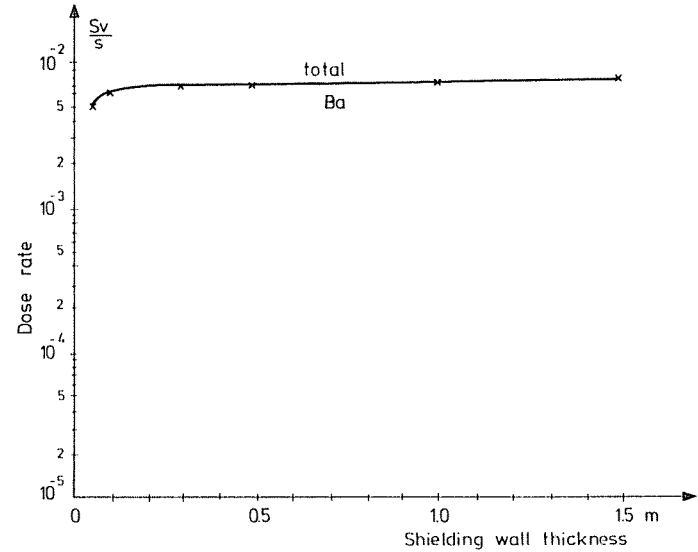
Fig. 14. Dose rate on the neutron source side of the iron-siderite concrete wall after 30 years operating life of the reactor, as a function of the shielding wall thickness (resting time = 1 year)
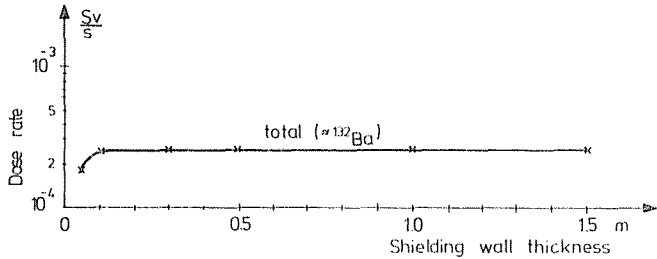
Fig. 15. Dose rate on the neutron source side of the iron-limonite concrete wall after 30 years operating life of the reactor as a function of the shielding wall thickness (resting time = 1 year)

Fig. 16. Dose rate on the neutron source side of the iron-hematite I concrete wall after 30 years operating life of the reactor as a function of the shielding wall thickness (resting time = 1 year)

Fig. 17. Dose rate on the neutron source side of the iron-himatite II concrete
wall after 30 years operating life of the reactor as a function of the shielding
wall thickness (resting time = 1 year)

Fig. 18. Dose rate on the neutron source side of the iron siderite concrete wall
after 30 years operating life of the reactor as a function of the shielding wall
thickness (resting time = 5 years)

Fig. 19. Dose rate on the neutron source side of the iron-limonite concrete wall after 30 years operating life of the reactor as a function of the shielding wall thickness (resting time = 5 years)
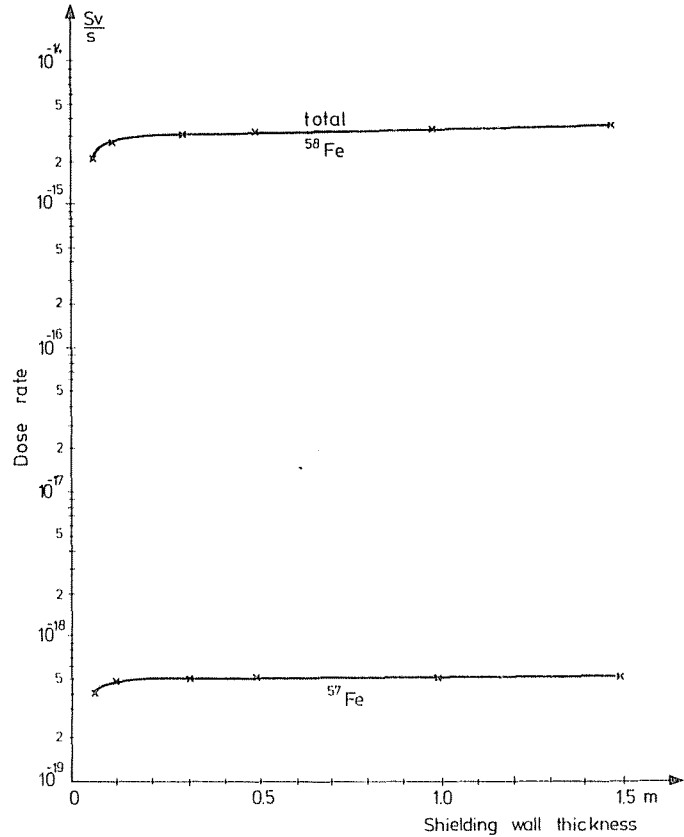
Fig. 20. Dose rate on the neutron source side of the iron-hematite I concrete wall after 30 years operating life of the reactor as a function of the shielding wall thickness (resting time = 5 years)
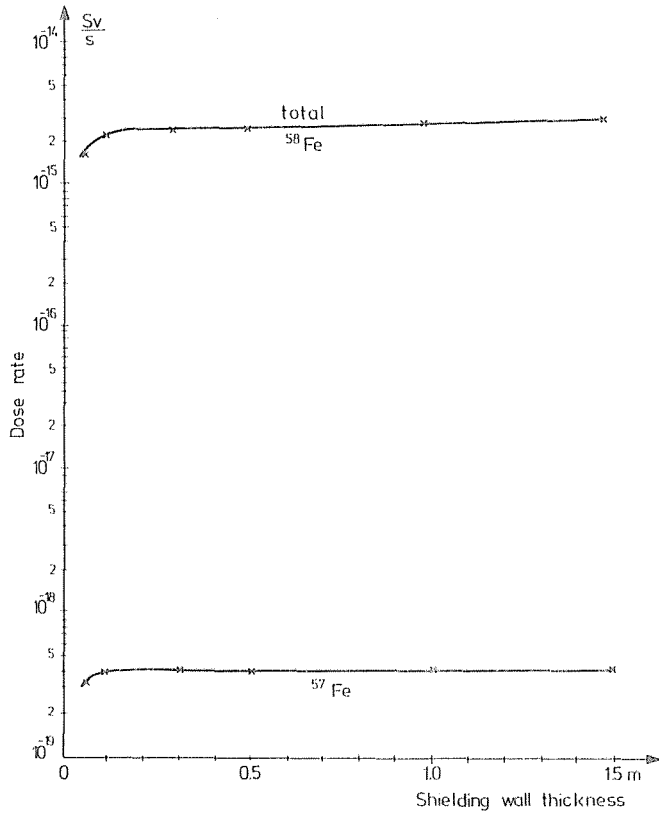
Fig. 21. Dose rate on the neutron source side of the iron-hematite II concrete wall after 30 years operating life of the reactor as a function of the resting time (saturation wall thickness)
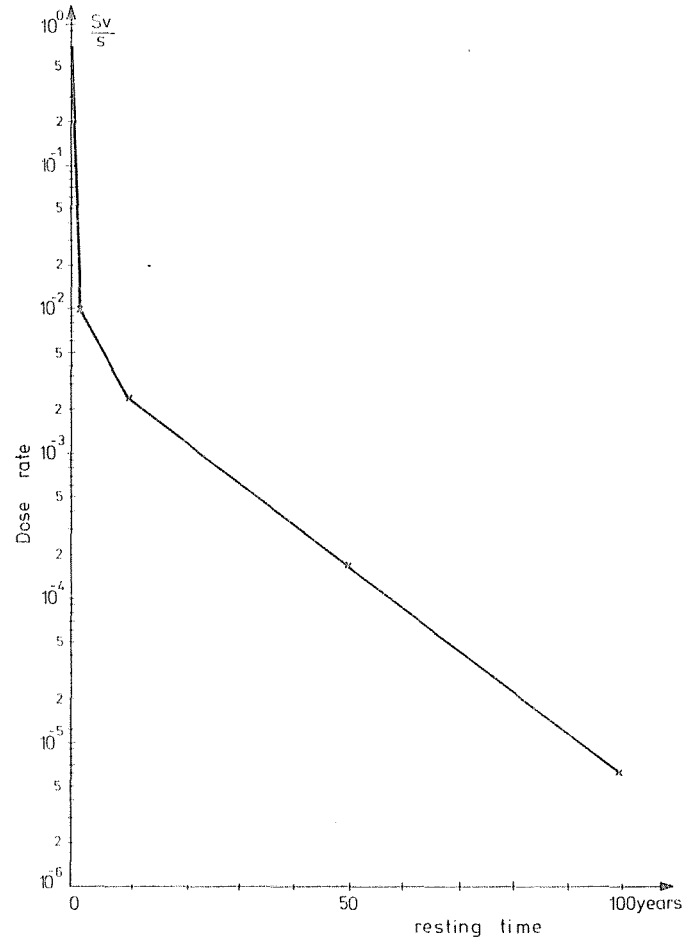
Fig. 22. Dose rate on the neutron source side of the iron-siderite concrete wall after 30 years operating life of the reactor as a function of the resting time (saturation wall thickness)
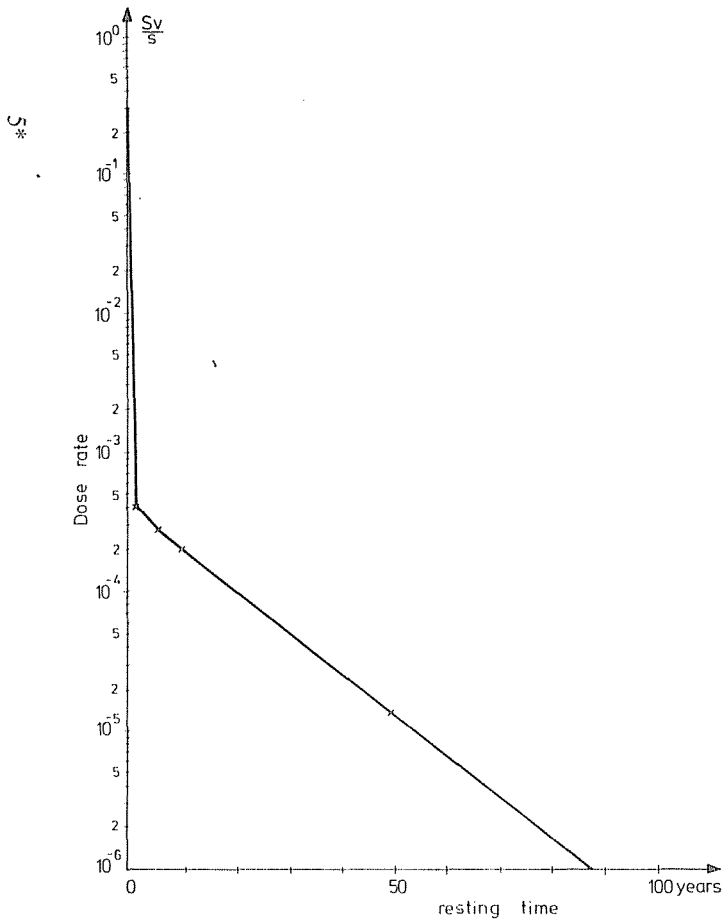
Fig. 23. Dose rate on the neutron source side of the iron-limonite concrete
wall after 30 years operating life of the reactor as a function of the resting time
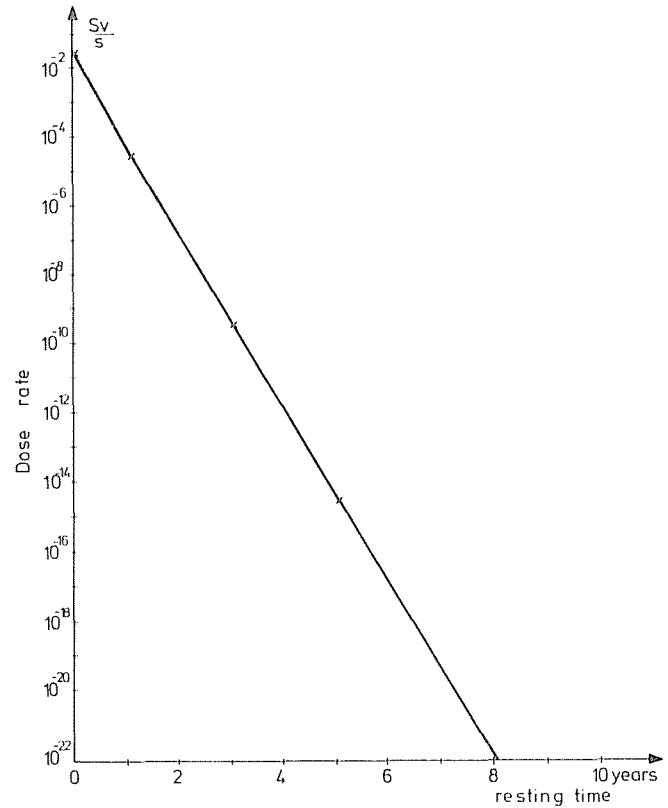(saturation wall thickness)

Fig. 24. Dose rate on the neutron source side of the iron-hematite I concrete
wall after 30 years operating life of the reactor as a function of the resting time
(saturation wall thickness)

Fig. 25. Dose rate on the neutron source side of the iron-hematite II concrete wall after 30 years operating life of the reactor as a function of the resting time (saturation wall thickness)
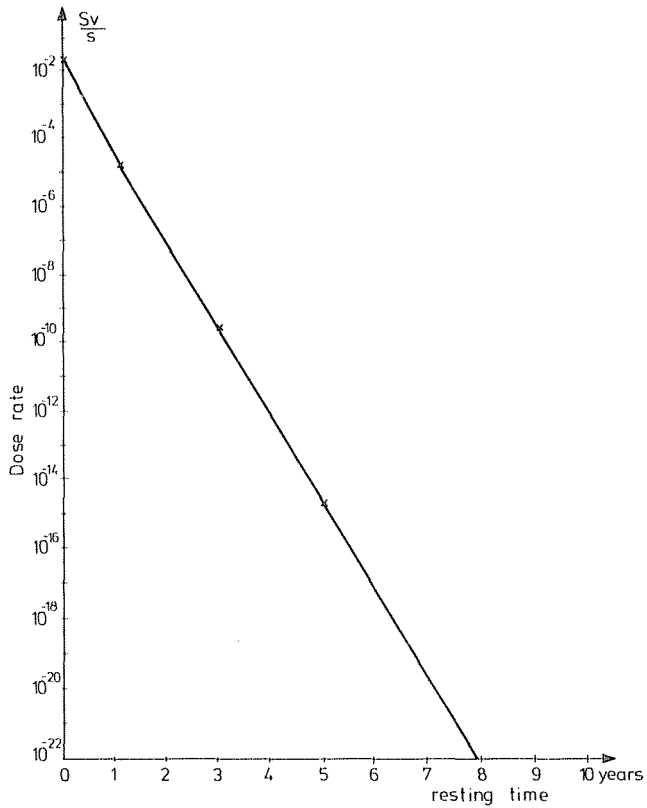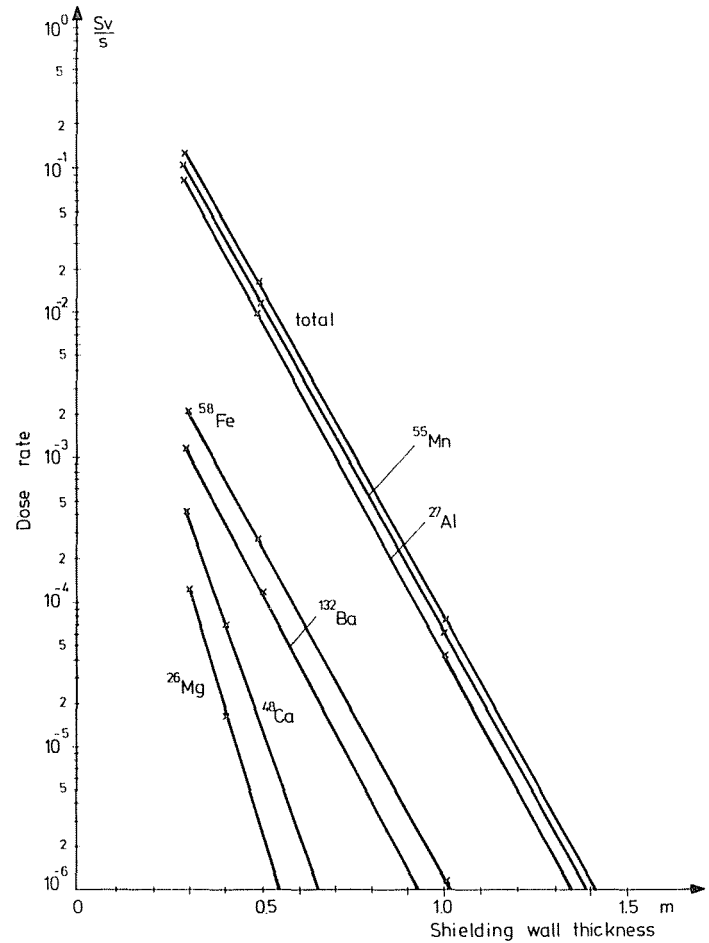
Fig. 26. Dose rate on the shielded side of the iron-siderite concrete wall after 30 years operating life of the reactor as a function of the shielding wall thickness (resting time = 0)
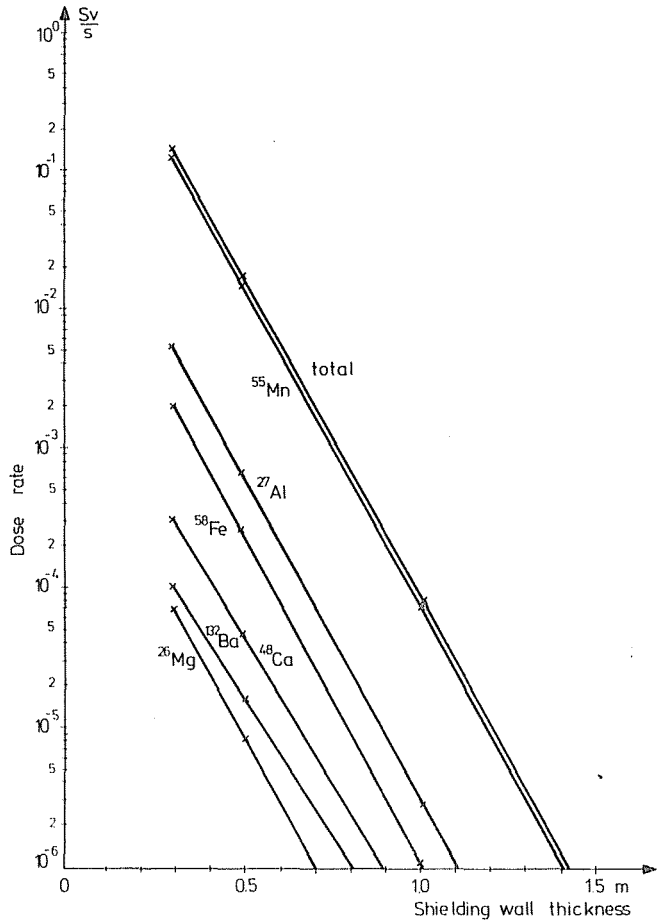
Fig. 27. Dose rate on the shielded side of the iron-limonite concrete wall after 30 years operating life of the reactor as a function of the shielding wall thickness (resting time = 0)
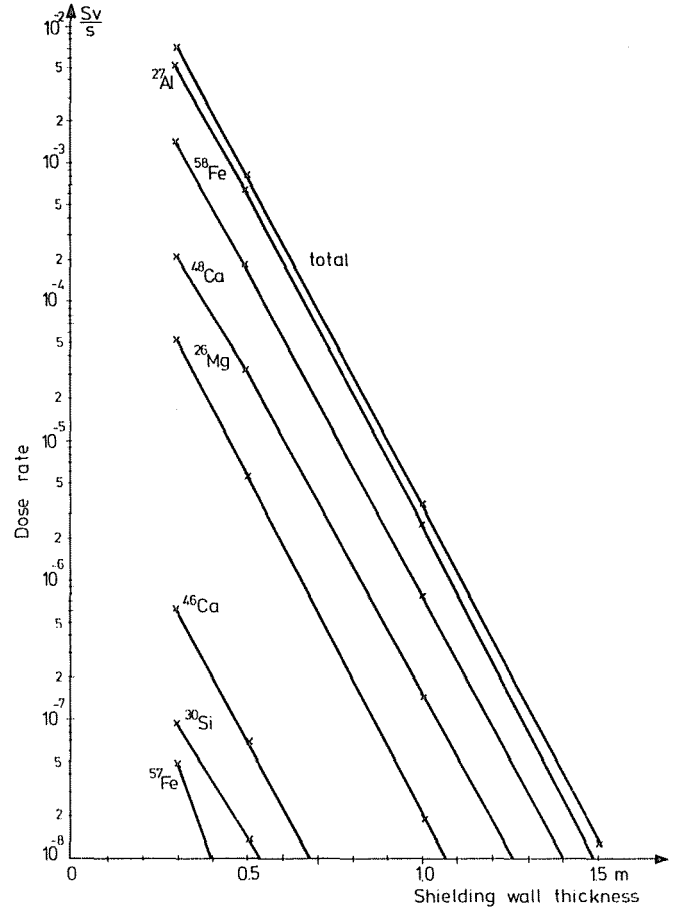

Fig. 28. Dose rate on the shielded side of the iron-hematite I concrete wall after 30 years operating life of the reactor as a function of the shielding wall thickness (resting time = 0)

Fig. 29. Dose rate on the shielded side of the iron-hematite II concrete wall after 30 years operating life of the reactor as a function of the shielding wall thickness (resting time = 0)
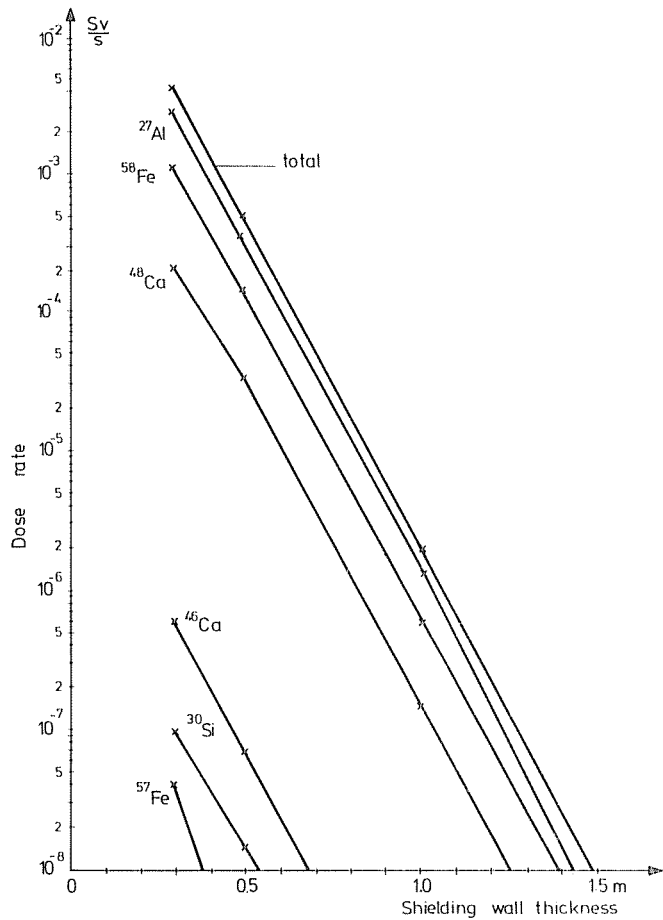
Fig. 30. Dose rate on the shielded side of the iron-siderite concrete wall after 30 years operating life of the reactor as a function of the resting time and the shielding wall thickness

Fig. 31. Dose rate on the shielded side of the iron-limonite concrete wall after 30 years operating life of the reactor as a function of the resting time and the shielding wall thickness

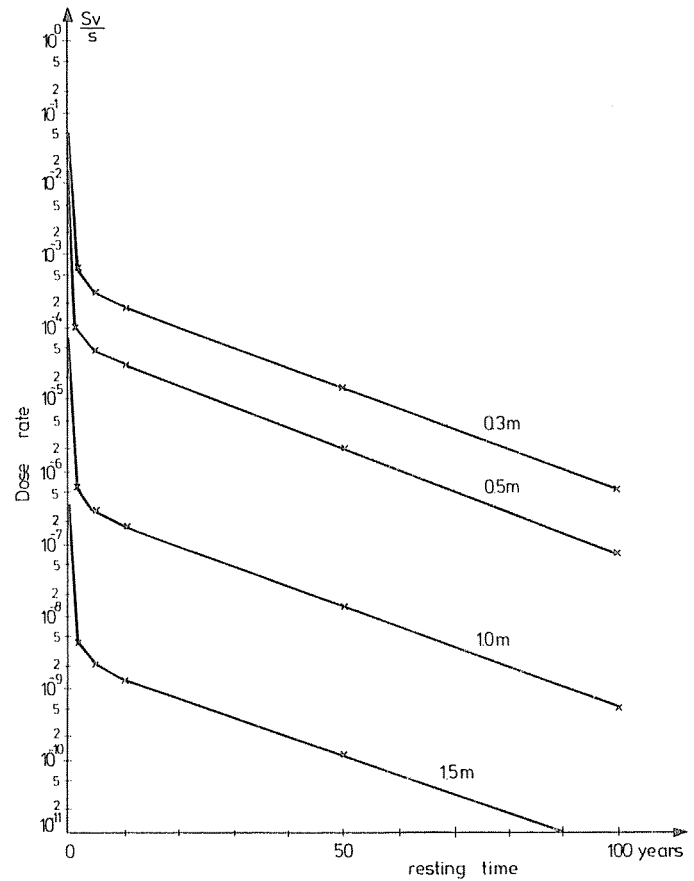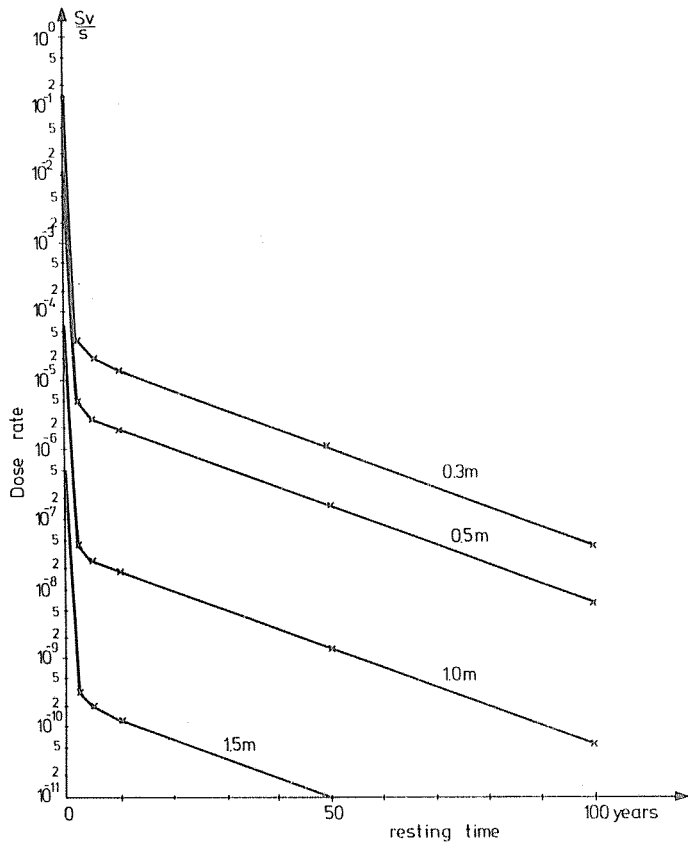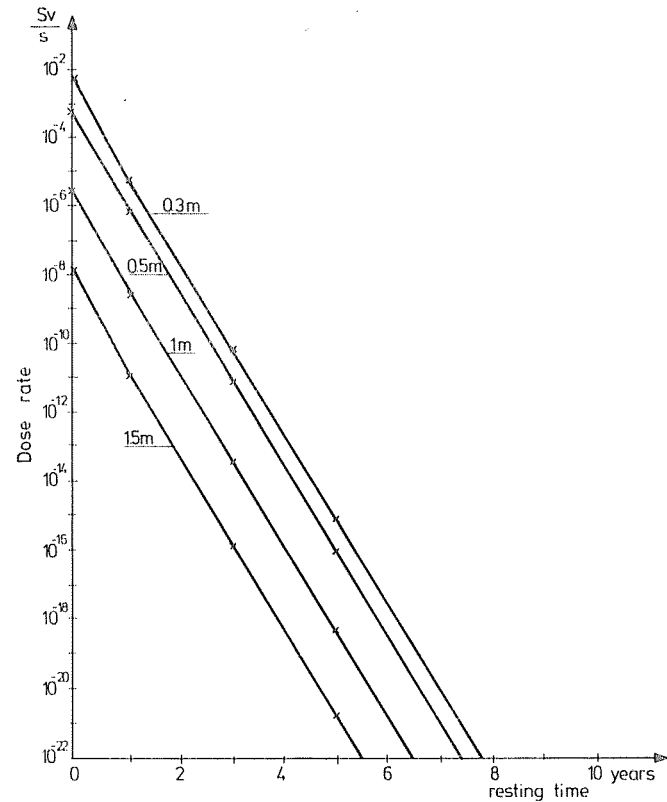*Fig. 32.* Dose rate on the shielded side of the iron-hematite I concrete wall after 30 years operating life of the reactor as a function of the resting time and the shielding wall thickness

3. Discussion

Activation and decay characteristics of four different shielding heavy concretes (iron-siderite, iron-hematite I and II, iron-limonite) were studied. The calculations were performed, as far as possible, with identical input data for all kinds of the concretes. Thus the results obtained can directly be compared and the following conclusions can be drawn:

1) The kinds of the trace elements and their concentration in the concretes investigated are very similar. This is an interesting result, because the aggregates used were deriving from different sources (see Table 2).

An important difference in the elementary composition of the shielding concretes was detected in their barium and iron content (see Table 3), but this is due to the preliminary design. The lower iron concentration in case of the concrete iron-hematite II. compared to the iron-hematite I. is due to the use of the high density Brazilian hematite. In this case the quantity of the hematite (Fe_2O_3) was increased at the expense of the iron (steel shot).

2) The gamma dose rate on the neutron source side of the concrete walls shows a saturation character as a function of the shielding wall thickness (Figures 10—13). The saturation thickness is between 20 and 25 cm (800 —900 kg/m^2) for all the concretes in question, considering that their density values are near each other. Therefore the calculations referring to the neutron source side of the concrete walls were performed supposing a saturation thickness.

3) From the point of view of accessibility during the maintenance of the nuclear power plant the most advantageous activation properties were found for the iron-hematite concretes (Figures 4—5). The γ-dose rate on the neutron source side of the shielding wall in this case is about one order of magnitude or a factor of 20 lower than that one for the iron-siderite and the iron-limonite concretes, respectively (see Figures 2—5). The decay of the γ-dose rate after 5 days resting time will be determined for all the concretes by the ^{59}Fe isotope with a half life of 45 days, but the base level is given by the isotope ^{133}Ba. The half life of this radionuclide is 10.4 years, that is it is comparable to the life time of the nuclear power plant, and as a result its role is monotonously increasing during the operating life of the reactor. The latter is especially emphasized in case of the iron-siderite concrete containing 10.3% of barium (Fig. 2). The relatively low dose rate in case of the hematite concretes is due to the fact that the barium is practically missing from their composition.

4) The half life of the components (such as ^{28}Al, ^{59}Fe, ^{31}Si, ^{27}Mg, ^{43}Ca, ^{56}Mn, ^{131}Ba, ^{133}Ba, ^{135}Ba and ^{139}Ba, see Figs 6—9) determining the specific activity of the shielding concretes after a 30 years operation time of the nuclear power plant is between some minutes and some days (maximum 45 days for the ^{59}Fe), except the ^{133}Ba. Due to its long half life this isotope will determine the

activity of the shielding concrete after final shutdown of the reactor. The iron-hematite concretes do not contain barium, and as a result their specific activity is about one order of magnitude lower than that for the other concretes. Also the decay of the activity of the iron-hematite concretes is faster, due to the above mentioned reasons. The lowest specific activity was found in case of the concrete iron-hematite II, being 40—50 per cent lower than the one for the concrete iron-hematite I. This is due to its lower iron content (see Table 3.).

5) A trend, similar to the characteristics mentioned above can be observed in the γ-dose rates on the neutron source and shielded side of the concrete wall after 30 years operation life (see Figures 10—32.). From among the concrete components giving the highest contribution to the γ-dose rate — apart from the barium — the isotope ^{59}Fe has the longest half life (45 days), but also it decays practically in 1—5 years (see Figs 22—25., 30—32). Afterwards the change of the γ-dose rate will be determined by the decay of the ^{133}Ba isotope. As the iron-hematite concretes do not contain barium, their handling is much simpler and cheaper. Corresponding to its lower specific activity also the γ-dose rate is about 35 per cent lower on the neutron source side of the shielding wall for the concrete iron-hematite II than for the iron-hematite I (compare Figures 4—5 and 12—13). The smaller change in the γ-dose rate compared to the activity is due to the different spectral distribution of the γ-radiation of the different concrete components. That is why the shielding concretes have to be characterized from point of view of activation properties by the γ-dose rate instead of the specific activity [9—10].

6) The elementary composition of the steel shot aggregate was also investigated. From the results obtained (see Table 4) one can conclude that it had been produced of unalloyed steel.

Summarized: The most advantageous activation characteristics were found in case of the shielding concrete iron-hematite II. As the mechanical properties and shielding patameters of this concrete are also similar or better than the ones for the other concretes in question [5—7, 12, 13], this iron-hematite II concrete has been recommended to be used in the shielding structures of the Paks nuclear power plant.

Our results show, that the concretes used in the shielding structures of a nuclear reactor:

a) should not contain barium,

b) should have as low iron-content as it is possible,

c) should not contain iron aggregate in form of alloyed steel (that is unalloyed steel is only allowed).

As in most cases all these assumptions can not be fulfilled and lots of alloyed stainless steel structures have to be built in to the shielding walls of a power reactor, the use of a thin normal concrete wall in front of the actual heavy concrete shielding is recommended. (This idea has been more or less

realized by the heat-insulating concrete or water layers surrounding the reactor vessel [26]). The decay of the activity (and dose rate) for normal concrete is much faster — due to its short half life components — than in case of the heavy concretes discussed above [8]. Consequently, this solution ensures an easier and cheeper handling of the radiation shielding structures.

4. Acknowledgements

Summary

Activation and decay characteristics of 4 different kinds of heavy concretes were studied. First the elementary composition of the concretes was determined, afterwards calculations were performed by the computer code CAP [25] to determine the desired parameters. The results obtained for the different concretes were analysed and requirements of producing radiation shielding concretes with optimal activation characteristics were summarized.

References

1. IAEA, Decommissioning of nuclear facilities — A review of status, At. Energy Rev. *12*, 1, IAEA, Vienna (1974)
2. GLAUBERMAN, H. et al.: Technical and economic aspects of nuclear power plant decommissioning. In the proceedings of the Conference on Nuclear Power and its Fuel Cycle Vol. 4. p. 211. IAEA, Vienna, 1977
3. IAEA, Decommissioning of Nuclear Facilities, IAEA-179. Vienna (1975)
4. LUNNING, W. H.: Decommissioning of Nuclear Facilities. In the proceedings of the Conference on Nuclear Power and its Fuel Cycle, Vol. 4. p. 795, IAEA, Vienna, 1977
5. DÉSI, S.: Determination of shielding properties of radiation shielding heavy concretes (in Hungarian) BME-TR-41/76. BME-TR-41/76A, Budapest, 1976 (*)
6. DÉSI, S.: Determination of shielding properties of radiation shielding heavy concretes (in Hungarian) BME-TR-75/78 Budapest, 1978 (*)
7. NAGY, M.—DÉSI, S.: Determination of shielding properties of radiation shielding heavy concretes (in Hungarian) BME-TR-102/80 Budapest, 1980 (*)
8. ZSOLNAY, É.—SZONDI, E.: Investigation of activation properties of radiation shielding concretes (in Hungarian) BME-TR-68/77, Budapest, 1977 (*)
9. ZSOLNAY, É.—SZONDI, E.—CSOM, GY.—BEREZNAI, T.: Investigation of activation properties of radiation shielding heavy concretes (in Hungarian) BME-TR-80/78, Budapest, 1978 (*)
10. ZSOLNAY, É.—SZONDI, E.—CSOM, GY.: Investigation of activation properties of radiation shielding heavy concretes (in Hungarian) BME-TR-89/79, Budapest, 1979 (*)
11. ZSOLNAY, É.—SZONDI, E.—CSOM, GY.—BÓDIZS, D.: Investigation of activation properties of radiation shielding heavy concretes (in Hungarian) BME-TR-103/80, Budapest, 1980 (*)

(*) Reports for restricted distribution

12. BUDAY, T.: Concrete technology for radiation shielding heavy concretes (in Hungarian) Institute for Building Science Budapest (ÉTI), 34—2.886. Budapest, 1977
13. Personal communication of dr. T. BUDAY (Institute for Building Science, Budapest (ÉTI))
14. SIMONITS, A. et al., J. Radioanal. Chem. *24* (31) 1975
15. MAENHAUT, W. et al., J. Radioanal. Chem. *2* (325) 1971
16. SIMONITS, A. et al., J. Radioanal. Chem. *31* (467) 1976
17. Technical documentation of the Paks Nuclear Power Plant Part IX/I. (in Hungarian)
18. BUDAY, T.—TÓTH, L.: Radiation shielding concretes. Manuscript. Budapest, 1969
19. Handbook on Nuclear Activation Cross Sections. IAEA Techn. Rep. Ser. No. 156., 1974 Vienna
20. ERDTMANN: Neutron activation Tables Vol. 6 Verlag Chemie 1976
21. ERDTMANN: Die gamma-linien der Radionuclide I—II—III Jül-1003-AC, September 1973
22. W. L. ZIJP. Nuclear Data Guide for Neutron Metrology. a) Petten, 1977 b) Petten, 1979
23. E. GRAY (Ed.): American Institute of Physics Handbook. McGraw-Hill, New York, 1972
24. Personal communication of dr. T. BUDAY (Institute for Building Science, Budapest (ÉTI))
25. The computer program CAP (Calculation of Activation Properties). To be published.
26. R. G. JAEGER et al.: Engineering Compendium on Radiation Shielding Vol. I.—II.—III., Springer Verlag, Berlin 1968, 1970, 1975.

Éva M. ZSOLNAY
Dr. Gyula CSOM   H-1521 Budapest
Dr. Egon J. SZONDI